Published in final edited form as:
Am J Physiol Heart Circ Physiol. 2007 March ; 292(3): H1352–H1363. doi:10.1152/ajpheart.00065.2006.

Vasopressin stimulates action potential firing by protein kinase C-dependent inhibition of KCNQ5 in A7r5 rat aortic smooth muscle cells

Lioubov I. Brueggemann[1], **Christopher J. Moran**[1], **John A. Barakat**[1], **Jay Z. Yeh**[2], **Leanne L. Cribbs**[1], and **Kenneth L. Byron**[1]

1 *Department of Pharmacology and Experimental Therapeutics and Cardiovascular Institute, Loyola University Chicago, Maywood*

2 *Department of Pharmacology, Northwestern University, Chicago, Illinois*

Abstract

[Arg^8]-vasopressin (AVP), at low concentrations (10–500 pM), stimulates oscillations in intracellular Ca^{2+} concentration (Ca^{2+} spikes) in A7r5 rat aortic smooth muscle cells. Our previous studies provided biochemical evidence that protein kinase C (PKC) activation and phosphorylation of voltage-sensitive K^+ (K_v) channels are crucial steps in this process. In the present study, K_v currents (I_{Kv}) and membrane potential were measured using patch clamp techniques. Treatment of A7r5 cells with 100 pM AVP resulted in significant inhibition of I_{Kv}. This effect was associated with gradual membrane depolarization, increased membrane resistance, and action potential (AP) generation in the same cells. The AVP-sensitive I_{Kv} was resistant to 4-aminopyridine, iberiotoxin, and glibenclamide but was fully inhibited by the selective KCNQ channel blockers linopirdine (10 μM) and XE-991 (10 μM) and enhanced by the KCNQ channel activator flupirtine (10 μM). $BaCl_2$ (100 μM) or linopirdine (5 μM) mimicked the effects of AVP on K^+ currents, AP generation, and Ca^{2+} spiking. Expression of KCNQ5 was detected by RT-PCR in A7r5 cells and freshly isolated rat aortic smooth muscle. RNA interference directed toward KCNQ5 reduced KCNQ5 protein expression and resulted in a significant decrease in I_{Kv} in A7r5 cells. I_{Kv} was also inhibited in response to the PKC activator 4β-phorbol 12-myristate 13-acetate (10 nM), and the inhibition of I_{Kv} by AVP was prevented by the PKC inhibitor calphostin C (250 nM). These results suggest that the stimulation of Ca^{2+} spiking by physiological concentrations of AVP involves PKC-dependent inhibition of KCNQ5 channels and increased AP firing in A7r5 cells.

Keywords

potassium channel; signal transduction; membrane potential; calcium; vascular smooth muscle; M current

Vasoconstrictor hormones cause contraction of vascular smooth muscle (VSM) cells by increasing cytosolic free Ca^{2+} concentration ($[Ca^{2+}]_i$), which in turn activates the cells' contractile apparatus. Voltage-sensitive L-type Ca^{2+} channels are known to be important in vasoconstrictor action (27), although the signaling pathways leading to activation of L-type channels are not well characterized. Influx of Ca^{2+} via L-type channels is enhanced by

Address for reprint requests and other correspondence: K. L. Byron, Loyola Univ. Medical Center, Dept. of Pharmacology, 2160 South First Ave., Maywood, IL 60153 (e-mail: kbyron@lumc.edu).
Present address of C. J. Moran: William Beaumont Hospital, Royal Oak, MI 48073.

membrane depolarization, which may result from activation of nonselective cation currents (34,47,54) or Cl^- currents (30). Alternatively, inhibition of outward K^+ currents could provide a depolarizing stimulus for activation of L-type Ca^{2+} channels (38).

We have previously demonstrated that concentrations of [Arg^8]-vasopressin (AVP) that may be found in the systemic circulation (10–500 pM) modulate the frequency of L-type Ca^{2+} channel-dependent Ca^{2+} spikes in A7r5 rat aortic smooth muscle cells. The stimulation of Ca^{2+}-dependent action potentials, which underlie AVP-stimulated Ca^{2+} spiking, involves activation of a novel signaling pathway (5). Treatment of A7r5 cells with 100 pM AVP leads to increased tyrosine phosphorylation of Kv1.2 delayed rectifier K^+ channels (3). We previously speculated (3) that tyrosine phosphorylation of Kv1.2 channels inhibits their function and thereby induces the membrane depolarization that is required for L-type Ca^{2+} channel activation.

The signal transduction pathway leading to Kv1.2 phosphorylation and Ca^{2+} spiking requires activation of protein kinase C (PKC) (3,14). The present study provides the first electrophysiological evidence that activation of PKC at physiological concentrations of AVP leads to inhibition of an outward voltage-sensitive K^+ current, depolarizes the membrane, and induces action potential generation in vascular smooth muscle cells. This mechanism may be of fundamental importance to understanding how vasoconstrictor hormones regulate vascular smooth muscle excitability.

The identity of the K^+ channels involved in the actions of AVP may be inferred from the electrophysiological and pharmacological characteristics of the K_v current that is inhibited. These characteristics do not match those expected of Kv1.2 channels, but rather fit the known properties of KCNQ channels, a family of K_v channels whose best known roles are as mediators of the "M current," a slowly activating, delayed rectifier K^+ current targeted by acetylcholine in the regulation of neuronal excitability. Although KCNQ channels have no previously identified role in vasoconstrictor actions, we have detected expression of KCNQ5 in A7r5 cells and in isolated rat aortic smooth muscle and provide evidence that these channels are targeted in a PKC-dependent manner by physiological vasoconstrictor concentrations of AVP.

MATERIALS AND METHODS

Patch clamp

A7r5 cells grown to confluence in cell culture as described previously (5) were trypsinized and replated on glass coverslips. Within 4 h of replating, the whole cell perforated-patch configuration was used to measure membrane currents under voltage-clamp conditions and membrane potentials under current-clamp conditions in single cells. All experiments were performed at room temperature with continuous perfusion of bath solution. Resistances of patch pipettes were 1.5–2.5 MΩ after being filled with internal solutions. Series resistance was not compensated.

The standard bath solution contained (in mM) 5 KCl, 130 NaCl, 10 HEPES, 2 $CaCl_2$, 1.2 $MgCl_2$, and 5 glucose, pH 7.3. Standard internal (pipette) solution contained (in mM) 110 K-gluconate, 30 KCl, 5 HEPES, 1 K_2EGTA, and 2 Na_2ATP, pH 7.2. Osmolality was adjusted to 268 mosmol/l with D-glucose. Amphotericin B (200 μg/ml) in internal solution was used for membrane patch perforation. Experiments in whole cell perforated-patch configuration were started with series resistance (R_s) below 30 MΩ; cells with an abrupt decrease in R_s were discarded. Stable control currents were recorded for 10–20 min before bath application of pharmacological agents.

Voltage-clamp command potentials were generated using an Axo-patch 200B amplifier under control of pCLAMP8 software. Currents were recorded by application of 1- or 5-s voltage steps from a −74-mV holding potential to test potentials ranging from −94 to −46 mV. Voltage commands were applied every 5 or 10 s; results were then normalized to the membrane capacitance. Whole cell currents were digitized at 10 kHz and filtered at 1 kHz for 1-s voltage step duration and digitized at 2 kHz and filtered at 200 Hz for 5 s voltage step duration. We averaged 1,000 points (corresponding to 100-ms recording time with a 1-s voltage step or 500-ms recording time with a 5-s voltage step) to obtain end-pulse steady-state K^+ current. Whole cell capacitance was compensated. Leak subtraction was performed for some experiments (see legends) by extrapolation of the linear portion of the current-voltage (*I-V*) curve negative to −69 mV as described by Passmore et al. (40). Liquid junction potentials were calculated using Junction Potential Calculator provided by pCLAMP8 software and subtracted off-line. To analyze the voltage dependence of channel activation, we fitted the conductance calculated from the tail currents (measured at −30 mV after steps from −74 mV to voltages between −94 and +36 mV) with a Boltzmann distribution: $G/G_{max} = 1/[1 + \exp(V_{0.5} - V)/s]$, where G/G_{max} is fractional maximal conductance, $V_{0.5}$ is the voltage of half-maximal activation, and *s* is the slope factor.

Current-clamp recording of membrane potential was performed in current-clamp fast mode with $I = 0$ pA. Data are presented as means ± SE. For comparisons between two groups, Student's *t*-test, paired or unpaired as appropriate, was used for statistical analysis, with *P* values <0.05 considered statistically significant.

$[Ca^{2+}]_i$ measurements

Essentially as described previously (5,6), A7r5 cells were grown to confluence on glass coverslips or six-well plates. The cells were washed twice with control medium (135 mM NaCl, 5.9 mM KCl, 1.5 mM $CaCl_2$, 1.2 mM $MgCl_2$, 11.5 mM glucose, and 11.6 mM HEPES, pH 7.3) and then incubated in the same medium with 2 μM fura-2 AM, 0.1% bovine serum albumin, and 0.02% Pluronic F127 detergent for 90–120 min at room temperature (20–23°C) in the dark. The cells were then washed twice and incubated in the dark in control medium for 1–5 h before the start of the experiment. Fura-2 fluorescence (at 510 nm) was measured in cell populations at room temperature with a Perkin-Elmer Life Sciences LS50B fluorescence spectrophotometer or a BioTek fluorescence plate reader. Background fluorescence was recorded before cells were loaded with fura-2 (6-well plates) or determined at the end of the experiment by quenching the fura-2 fluorescence for 10–15 min in the presence of 5 μM ionomycin and 6 mM $MnCl_2$ in Ca^{2+}-free medium (coverslips). After background fluorescence was subtracted, the ratio of fluorescence at 340-nm excitation to that at 380 nm was calculated and calibrated in terms of $[Ca^{2+}]_i$.

Calibration of fura-2 fluorescence in terms of $[Ca^{2+}]_i$ was carried out as described previously (4) using solutions of known Ca^{2+} concentration to construct a standard curve. The Ca^{2+} concentration of the standard solutions was calculated using software (MaxChelator, version 6.60) that accounts for binding of Ca^{2+} to each constituent of the solution. For analysis of fluorescence ratios recorded from cells, the equation $[Ca^{2+}]_i = K_d \cdot \beta \cdot [(R - R_{min})/(R_{max} - R)]$ (18) was fit to the standard curve (using SigmaPlot software; Systat Software, Point Richmond, CA) and used to convert ratios (R) into $[Ca^{2+}]_i$. In situ calibration of fura-2 fluorescence by direct determination of minimum and maximum ratios [R_{min} and R_{max}, respectively (18)] from within cells yields similar calibrated values. Traces shown are representative of at least three similar experiments.

RT-PCR

Total RNA was isolated from either A7r5 cells or endothelium-denuded rat aortas using RNeasy mini kit (Qiagen) plus DNase treatment. cDNA was synthesized with iScript cDNA synthesis kit (Bio-Rad), and then one-tenth of the cDNA product was used for PCR. PCR was carried out using Platinum PCR Supermix (Invitrogen) and 10 pmols of forward and reverse primers at the appropriate annealing temperature (dependent on primer pair). Primers were adapted from Ohya et al. (Ref. 39; KCNQ1–3, KCNQ5) and Beisel et al. (Ref. 1; KCNQ4). A portion of the PCR reaction product was run on 0.8% agarose-TBE (Tris-borate-EDTA) gel against a 100-bp ladder as a molecular weight marker (New England Biolabs). Minus-RT controls using the same reaction conditions with A7r5 RNA were negative for all KCNQ primer pairs (not shown). Expected sizes of reaction products are as follows: KCNQ1, 453 bp; KCNQ2, 372 bp; KCNQ3, 424 bp; KCNQ4, 495 bp; and KCNQ5, 240 bp. Products were excised from the gel, purified using the Qiaquick gel purification kit (Qiagen) and cloned into pCR 2.1 vector using a TA cloning kit (Invitrogen) before DNA was sequenced for confirmation. Rat brain RNA was used as a positive control for each primer set.

RNA interference

A short-hairpin RNA (shRNA) lentivirus targeted to the rat KCNQ5, lv-GFP_KCNQ5_shRNA, was constructed using target sequences derived from the predicted KCNQ5 mRNA coding sequence (GenBank accession no. XM_237012), with the assistance of BLOCK-iT RNAi Designer (Invitrogen). Oligonucleotides encoding the 29-nt hairpin target sequence (5′-TCAAGTTGACAGTGGCGGCTACAGAACAG-3′) were obtained commercially (Invitrogen), annealed, and cloned into the pSIH1-H1-Puro shRNA lentivirus vector (System Biosciences). The vector is designed to coexpress copGFP protein, a monomeric green fluorescent protein (GFP) cloned from the copepod, *Pontellina plumata*. Replication-deficient shRNA lentivirus was prepared using the pPACK-H1 Lentivector packaging system and 293 TN producer cell line according to the manufacturer's protocol. Adherent A7r5 cells in culture were infected with lv-KCNQ5_shRNA by using Polybrene (hexadimethrine bromide; Sigma). Five to seven days later, GFP-positive cells were chosen for electrophysiological recordings. A GFP control lentivirus, lv-GFP, was constructed in parallel with pPACK-H1 reagents and was used to infect A7r5 cells for control recordings.

Immunohistochemical detection of KCNQ5

A7r5 cells were subcultured on 12-mm round glass coverslips and infected with lv-GFP_KCNQ5_shRNA as described above. The cells were fixed with 2% paraformaldehyde in phosphate-buffered saline (PBS; 138 mM NaCl, 2.7 mM KCl, 8.1 mM Na_2HPO_4, and 1.2 mM KH_2PO_4, pH 7.4) for 15 min, washed twice with PBS, and permeabilized with 0.5% Triton X-100 (Sigma) in PBS for 15 min. After being washed with 0.1% Triton X-100 in PBS, coverslips were blocked with Image-iT FX signal enhancer (Molecular Probes, Eugene, OR) according to the manufacturer's instructions for 30 min, followed by an additional 2-h blocking step with 10% goat serum. Coverslips were washed three times with 0.1% Triton X-100 in PBS and incubated with rabbit polyclonal anti-KCNQ5 antibodies (Chemicon International, Temecula, CA) at a 1:500 dilution for 2 h at room temperature. After three washing steps with 0.1% Triton X-100 in PBS for 15 min each, coverslips were incubated for 2 h at room temperature in the dark with Alexa Fluor 594 goat anti-rabbit IgG secondary antibody (1:400 dilution in 0.1% Triton X-100 plus 10% goat serum in PBS). Three additional washing steps for 15 min with 0.1% Triton X-100 in PBS were performed before coverslips were mounted on glass slides using the SlowFade light antifade kit (Molecular Probes). Cell images were acquired using C Imaging System (Compix) with an Olympus 1X71 inverted epifluorescence microscope (×10 fluorescent objective) and Simple PCI software (version 5.3.1). Two images of each field were captured, at 490-nm excitation wavelength for GFP fluorescence and at 595-

nm excitation wavelength for Alexa Fluor 594 fluorescence, respectively. Regions of interest were defined by outlining cells expressing or not expressing GFP fluorescence (identified using 490-nm excitation). Digital images captured using 595-nm excitation were analyzed for mean pixel intensity of regions of interest. Coverslips incubated without primary antibody had no detectable fluorescence with 595-nm excitation (results not shown).

Materials

Cell culture media were obtained from GIBCO-BRL (Gaithersburg, MD) or MediaTech (Herndon, VA). Fura-2 AM, fura-2 pentapotassium salt, and Pluronic F127 were obtained from Molecular Probes. 4β-Phorbol 12-myristate 13-acetate (PMA) was obtained from Calbiochem (San Diego, CA). Correolide was generously provided by Merck Research Laboratories (Rahway, NJ).

RESULTS

To evaluate the hypothesis that the previously observed phosphorylation of K_v channels in A7r5 cells is associated with a reduction of outward K_v currents, we utilized whole cell perforated-patch clamp techniques to measure K_v currents. Under physiological ionic conditions similar to those used for previous Ca^{2+} spiking studies, a voltage step protocol was applied to simultaneously record inward currents through L-type Ca^{2+} channels (I_{CaL}, at the beginning of the pulse) and outward current through K^+ channels (after inactivation of L-type currents at the end of the pulse). As shown in Fig. 1, by stepping to different voltages, a typical inward I_{CaL} was detected at the beginning of the pulse, which reached a mean peak at +1 ± 1.3 mV (n = 13), whereas an outwardly rectifying current developed after a delay, reaching a steady-state level at the end of the pulse. The amplitude of the initial inward current and the amplitude of the delayed outward current are plotted in Fig. 1*C* to depict the *I-V* relationships. The delayed outward current component is likely to be a mix of currents, but the reversal potential (E_{rev}) of outward current at −51.4 ± 3.1 mV (n = 16) indicates that K^+ is the predominant current carrier under these ionic conditions. In support of this contention, increasing external [K^+] from 5 to 140 mM induced a shift in E_{rev} of the outward current from −49.4 ± 5.5 to −8.4 ± 1.9 mV (n = 4, data not shown). Increased variability of outward currents at positive potentials may reflect an increased contribution of Ca^{2+}-activated K^+ currents (I_{KCa}) following Ca^{2+} influx through L-type Ca^{2+} channels.

A 10-min exposure to 100 pM AVP, a concentration shown in previous studies to stimulate repetitive Ca^{2+} spiking in these cells, significantly inhibited the outward K^+ current at membrane potentials between −44 and −14 mV (74% inhibition on average over this voltage range, n = 5) but had no effect on I_{CaL} (Fig. 1, *B* and *C*). Action potential firing, the electrophysiological equivalent of Ca^{2+} spiking, was observed in the same cells by switching to current-clamp recording conditions (Fig. 1*D*).

Whole cell current-clamp recordings revealed that 100 pM AVP induced a gradual depolarization of the membrane, which eventually triggered repetitive action potential firing with a mean latency of 5.7 ± 0.8 min (n = 6, Fig. 2*A*).

Membrane depolarization might occur either by activation of inward currents (e.g., Na^+, Ca^{2+}, Cl^-) or by inhibition of outward K^+ currents. Activation of inward currents would decrease membrane resistance, whereas inhibition of K^+ currents would increase membrane resistance. We found that AVP significantly increased membrane resistance (from 1.44 ± 0.27 to 2.26 ± 0.41 GΩ, measured under voltage-clamp conditions before and 10 min after application of 100 pM AVP, n = 7, $P < 0.005$; Fig. 2). This effect was associated with a 10-mV depolarization of the membrane (from −55.9 ± 1.6 to −45.2 ± 1.4 mV, n = 8, $P < 0.001$) measured before action potential firing in the same cells.

If AVP stimulates Ca^{2+} spiking by inhibition of K^+ channels, one might predict that K^+ channel blockers would mimic the effects of AVP in A7r5 cells. As shown in Fig. 3*A*, $BaCl_2$, a nonselective K^+ channel blocker (49), stimulated Ca^{2+} spiking in A7r5 cells in a concentration-dependent manner, reminiscent of the effects of AVP (5). Moreover, 100 μM $BaCl_2$ also mimicked AVP in inhibiting outward K^+ currents without affecting the amplitude of L-type Ca^{2+} current (Fig. 3*B*) and triggered action potential firing in single A7r5 cells (Fig. 3*C*).

As noted above, outward currents recorded at positive test potentials may reflect a contribution of I_{KCa} following Ca^{2+} influx through L-type Ca^{2+} channels. To examine the regulation of K_v currents more specifically, we used a combination of verapamil, a Ca^{2+} channel blocker, and iberiotoxin, a blocker of large-conductance Ca^{2+}-activated K^+ channels (BK_{Ca}) to record K_v currents in isolation from L-type Ca^{2+} currents and I_{BKCa} currents. Including 10 μM verapamil and 100 nM iberiotoxin in the external solution abolished the inward L-type currents and diminished a component of the outward K^+ current (Fig. 4*A*). An outwardly rectifying K_v current remained in the presence of the verapamiliberiotoxin cocktail. To rule out additional contributions of iberiotoxininsensitive, Ca^{2+}-activated K^+ currents (53,57,59) that may be activated by verapamilinsensitive Ca^{2+} influx, we tested the effects of gadolinium (Gd^{3+}), a cation channel blocker that effectively inhibits Ca^{2+} influx via both voltage-sensitive Ca^{2+} currents and nonselective cation currents. There was no significant reduction of the remaining K_v current when verapamiliberiotoxin was replaced by 100 μM Gd^{3+} (Fig. 4*A*) or when iberiotoxin was added following Gd^{3+} (Fig. 5*A*), suggesting that blocking Ca^{2+} influx with Gd^{3+} is sufficient to prevent activation of I_{KCa} and effectively isolates K_v currents from other contaminating currents (Fig. 4, *A*–*C*). Under these conditions, a normalized conductance-voltage plot was well fit by a single Boltzmann curve with a $V_{0.5} = -38 \pm 1.6$ mV and a slope $s = 8.3 \pm 0.4$ mV (Fig. 4*D*). The isolated I_{Kv} recorded in the presence of Gd^{3+} may account for the AVP-inhibited outward current under physiological conditions (Fig. 1), because it was inhibited by 100 pM AVP with a time constant of 6.1 ± 1.1 min (Fig. 4, *E* and *F*).

To investigate the extent to which different kinds of K^+ channels contribute to the AVP-sensitive K_v current, we tested several relatively selective pharmacological agents that are often used to distinguish among K^+ channel classes. Treatment of A7r5 cells with 100 nM iberiotoxin, a specific inhibitor of BK_{Ca} channels, did not inhibit the AVP-sensitive K^+ current (Fig. 5*A*) and did not induce depolarization of membrane potential or trigger Ca^{2+} spiking (not shown). Although glibenclamide (10 μM), a selective inhibitor of ATP-sensitive K^+ channels, significantly reduced K^+ currents at positive voltages (by ~20%; Fig. 5*B*), it did not inhibit current over the physiological range of resting membrane potentials and did not activate Ca^{2+} spiking in A7r5 cells (not shown), suggesting a nonessential contribution of ATP-sensitive channels to the resting K^+ current. A relatively selective inhibitor of K_v channels, 4-aminopyridine (4-AP; 1 mM), induced a slight positive shift of activation voltage dependence without significant inhibition of the current (Fig. 5*C*). A nonspecific K^+ channel blocker, Ba^{2+} (100 μM), significantly inhibited ~70% of K^+ currents at negative potentials, with this value diminishing to ~40% as the membrane potentials were raised to +36 mV (Fig. 5, *D* and *E*). A specific Kv1 family inhibitor, correolide (1 μM) (15,21), significantly reduced K_v currents in A7r5 cells (by 52 ± 7%; Fig. 5*F*). Block of I_{Kv} by correolide was voltage independent, and there was no shift of the voltage activation curve (not shown). Unlike $BaCl_2$ (Fig. 3), correolide treatment did not stimulate Ca^{2+} spiking or action potential generation (not shown).

KCNQ or Kv7 family channels may contribute to K_v currents in vascular smooth muscle cells (39,60). We tested the effects of the selective KCNQ channel blockers linopirdine (100 μM) and XE991 (10 μM) and found that both agents significantly inhibited I_{Kv} in A7r5 cells (Fig. 5, *G* and *H*). We also found that I_{Kv} was significantly and reversibly enhanced by 10 μM flupirtine, a KCNQ channel activator (Fig. 5*I*).

Measuring the time course of inhibition of I_{Kv} by 10 μM linopirdine revealed that within 15 min of addition of linopirdine, the AVP-sensitive current was fully inhibited such that addition of 100 pM AVP had no further effect (Fig. 6, *A* and *B*). The functional effects of KCNQ channel inhibition on A7r5 cell excitability were also examined using current clamp in single A7r5 cells. Treatment of A7r5 cells with 10 μM linopirdine resulted in repetitive action potential firing (Fig. 6*C*). In fura-2-loaded A7r5 cell monolayers, linopirdine (5 μM) stimulated Ca^{2+} spiking (Fig. 6*D*) and flupirtine (10 μM) transiently inhibited AVP-stimulated Ca^{2+} spiking (Fig. 6*E*).

To identify the subtypes of KCNQ channels that may be expressed in A7r5 cells, we prepared mRNA from A7r5 cells or isolated smooth muscle from rat thoracic aorta and performed RT-PCR using primers selective for each of the known KCNQ family members (KCNQ1–5). Rat brain mRNA served as a positive control for each KCNQ subtype. KCNQ5 was detected in both A7r5 cells and rat aorta (Fig. 7). KCNQ1 was also expressed in aorta but not in A7r5 cells; neither A7r5 cells nor aorta detectably expressed KCNQ2–4.

RNA interference techniques were used to knock down expression of KCNQ5 in A7r5 cells. We constructed a lentiviral vector for expression of a KCNQ5 shRNA (lv-GFP_KCNQ5-shRNA) with coexpression of GFP. Infection of A7r5 cells with lv-GFP_KCNQ5-shRNA resulted in ~20–30% of the cell population exhibiting GFP fluorescence 5–7 days after infection. Immunofluorescence staining revealed a significant reduction in KCNQ5 immunoreactivity in GFP-expressing cells compared with non-GFP-expressing cells in the same culture (Fig. 8, *A* and *B*). Whole cell patch clamp of the lv-GFP_KCNQ5-shRNA-infected fluorescent cells revealed that I_{Kv} was significantly smaller than that recorded from fluorescent cells infected with a GFP control virus (lv-GFP; Fig. 8*C*).

KCNQ channels, and KCNQ5 in particular, may be regulated by activation of protein kinase C (11). We have previously presented evidence that PKC activation is a necessary step in the stimulation of Ca^{2+} spiking by AVP (14). Direct activation of PKC with PMA was shown to be effective in stimulating Ca^{2+} spiking (3,14). To test the hypothesis that inhibition of K_v currents may be a consequence of PKC activation, we examined the effects of PMA on I_{Kv}. We found that PMA mimicked AVP in inhibition of K_v currents (Fig. 9*A*). Furthermore, pretreatment with the PKC inhibitor calphostin C (250 nM) prevented the inhibition of I_{Kv} by 100 pM AVP (Fig. 9*C*). The same treatment with calphostin C was previously found to prevent AVP-stimulated Ca^{2+} spiking (14).

DISCUSSION

The present study is the first to examine effects of physiological concentrations of AVP on K^+ currents in vascular smooth muscle cells under conditions in which action potentials are induced in the same single cells. Our results confirm that sustained outward K^+ currents in A7r5 cells are inhibited in response to physiological concentrations of AVP and that this results in membrane depolarization and firing of action potentials. Importantly, this effect appears to be mediated by KCNQ5 channels, which have not been previously identified as a target for vasoconstrictor hormones. PKC activation is both necessary and sufficient to induce this response. We propose that this mechanism (PKC-dependent KCNQ channel inhibition and repetitive firing of Ca^{2+}-dependent action potentials) underlies the stimulation of Ca^{2+} spiking by AVP in A7r5 cells and may account for the physiological vasoconstrictor effects exerted by the low concentrations of AVP found in the systemic circulation.

The ability of vasoconstrictor hormones to stimulate arterial vasomotion (rhythmic constrictions of resistance arteries) has been recognized for several decades. These constrictions are associated with action potential firing in the vascular smooth muscle cells of

the artery wall (17). The presumed mechanism underlying the stimulation of action potential firing is a depolarization of the smooth muscle cell plasma membrane (sarcolemma) to a threshold potential at which the regenerative opening of voltage-sensitive Ca^{2+} channels would produce the steeply rising phase of the action potential. The entry of Ca^{2+} into the cytosol would then result in activation of the cell's contractile apparatus.

Membrane depolarization generally involves alterations in transmembrane ion fluxes. Vasoconstrictor hormones may positively or negatively affect a variety of ion channels, including voltage-sensitive Ca^{2+} channels, nonselective cation channels, K^+ channels, and Cl^- channels. The physiological ionic conditions in the cytosol and extracellular environment of vascular smooth muscle cells dictate that depolarization of the membrane from its resting potential would most readily occur by either an increase in Ca^{2+}, Na^+, or Cl^- permeability or a decrease in K^+ permeability of the sarcolemma.

Vasoconstrictor-induced membrane depolarization is often attributed to increased inward current. Inward Cl^- currents (due to Cl^- efflux) are enhanced by α-adrenergic stimulation in rabbit portal vein myocytes (13), by endothelin-1 or angiotensin II in rat pulmonary artery myocytes (20,45,46), and by endothelin-1 or vasopressin in A7r5 cells (56). Furthermore, the stimulation of Cl^- efflux has been implicated in the vasoconstrictor effects of endothelin-1 in rabbit basilar artery (10) and norepinephrine in rat resistance arteries (33) and aorta (32). There also is abundant evidence that vasoconstrictor hormones, including AVP, may enhance inward currents via stimulation of nonselective cation channel activity (Ca^{2+} and/or Na^+ influx) in vascular smooth muscle cells (for reviews, see Refs. 34,47,54), including A7r5 cells (26,29, 31,37,58). In most cases these effects have been evaluated using agonist concentrations that are orders of magnitude higher than would be found in the systemic circulation under physiological conditions.

Depolarization due to activation of inward currents (e.g., via Cl^- or nonselective cation channel activation) would be associated with a decrease in membrane resistance. In contrast, inhibition of K^+ currents would favor an increase in membrane resistance. It is noteworthy that we have observed a net increase in membrane resistance in the response to 100 pM AVP in the present study. This finding is consistent with our hypothesis that inhibition of K_v currents is the primary mechanism for membrane depolarization and stimulation of action potential firing by physiological concentrations of AVP in A7r5 cells.

There are reports that other vasoconstrictor agonists inhibit K^+ currents in vascular smooth muscle cells. For example, several earlier studies suggested that endothelin-1 inhibits K_v channels in arterial myocytes (2,36,46,51,52). The contribution of this effect to endothelin-1-induced membrane depolarization is not clear, however. In rabbit pial arteriolar myocytes exposed to varying concentrations of endothelin-1, membrane depolarization was associated with a decrease in membrane resistance ($EC_{50} \approx 100$ pM for both depolarization and decreasing membrane resistance; Ref. 19), suggesting that inhibition of K^+ channels was not the predominant depolarizing mechanism. Angiotensin II (100 nM) has been reported to decrease K_v currents in rabbit portal vein myocytes (8) and rat mesenteric arterial myocytes (24) by a PKC-dependent mechanism, although the contributions of this mechanism to membrane depolarization or Ca^{2+} signaling at physiological concentrations of angiotensin II have not been examined.

Inhibition of outward K^+ currents would suffice to depolarize the membrane, but in addition it also may serve to sensitize the cells to depolarization by small increases in inward current. According to Ohm's law, voltage is proportional to the product of current and resistance. Therefore, an increase in resistance would enable a small current to produce a larger change in voltage. In other words, inhibiting K^+ currents may render the cells more excitable such that

a small injection of inward current (e.g., by activation of inward Cl^- or cation currents) would more effectively depolarize the cells to activate L-type voltage-sensitive Ca^{2+} channels. Activation of L-type Ca^{2+} channels also would be more likely to produce a regenerative depolarization (action potential), because each channel opening would provide a larger depolarization when membrane resistance is increased.

Our studies have implicated K_v channels in the AVP signal transduction cascade. However, other classes of K^+ channels also are expressed in vascular smooth muscle cells, including inward rectifier (K_{ir}), Ca^{2+}-activated (K_{Ca}), and ATP-sensitive K^+ (K_{ATP}) channels [reviewed by Nelson and Quayle (38)]. Although there is evidence from numerous studies that vasoconstrictor agonists also may regulate these other types of K^+ channels, they are unlikely to be responsible for the effects of AVP observed in the present study. K_{Ca} channels are unlikely to be active in unstimulated cells, where resting $[Ca^{2+}]_i$ is typically <100 nM (5). It is unlikely therefore that inhibition of K_{Ca} currents would depolarize the membrane under these conditions. Furthermore, we have found that treatment of A7r5 cells with 100 nM iberiotoxin, a specific inhibitor of BK_{Ca} channels, did not inhibit the AVP-sensitive K^+ current (Fig. 5*A*) and did not induce depolarization of membrane potential or trigger Ca^{2+} spiking. On the other hand, K_{Ca} channels may be activated by Ca^{2+} and/or voltage during the course of the action potential and therefore may play a role in the repolarization or afterhyperpolarization phases of the action potential. K_{ATP} channels are inhibited by normal cytosolic ATP concentrations and therefore also are expected to be minimally active in healthy unstimulated cells (38). A study by Dumont and Lamontagne (12) found no effect of glibenclamide, a K_{ATP} channel blocker, on AVP-induced contraction, and glibenclamide by itself did not induce contraction of unstimulated aortic rings. We also found no effect of glibenclamide on Ca^{2+} spiking in A7r5 cells but observed a small inhibition of K_v currents at positive membrane potentials (Fig. 5*B*). Finally, the current-voltage profile of K_{ir} is not consistent with the currents that we observed to be inhibited by AVP, which are outwardly rectifying.

Although often used as a selective K_v channel blocker, 1 mM 4-AP was not an effective inhibitor of K_v currents in A7r5 cells (Fig. 5, *C* and *D*). The effects of 4-AP on native vascular smooth muscle K_v currents are highly variable, with aortic myocytes being particularly insensitive (9, 55). Although higher concentrations of 4-AP have been tested in several vascular myocyte preparations (9), 5 mM 4-AP has been reported to have nonspecific effects attributed to changes in cytosolic pH when perforated-patch recording techniques are used (41).

Correolide, a selective Kv1 family inhibitor (15,21), significantly inhibited K_v currents in the present study but was ineffective in stimulation of Ca^{2+} spiking in A7r5 cells. The reasons for this apparent discrepancy are not immediately clear. Inhibition of I_{Kv} by 1 μM correolide was very gradual. About 50% inhibition of I_{Kv} was achieved only after 20–30 min, as observed for native rabbit pial arteriolar K_v currents (7). The relatively slow inhibition of I_{Kv} by correolide in A7r5 cells may have prevented the Ca^{2+} spiking response from developing, because of inactivation of L-type Ca^{2+} channels or other time-dependent adaptive responses of the cells. It also is possible that correolide has nonspecific effects that interfere with the Ca^{2+} spiking response.

Despite its partial inhibition by correolide, other pharmacological characteristics of the AVP-sensitive K_v current in A7r5 cells (sensitivity to 100 μM Ba^{2+}, insensitivity to 4-AP) do not fit the expected properties of Kv1 family channels. Ba^{2+}-sensitive, 4-AP-insensitive K^+ channels have been implicated in the control of membrane potential and vasoconstriction in rabbit renal arcuate arteries (42). In primary rat aortic smooth muscle cells in culture (23) and guinea pig mesenteric artery myocytes in situ (22), Ba^{2+}(0.5–1.0 mM) induced significant membrane depolarization, increased membrane resistance, and induced repetitive action potential

generation. These effects have been attributed to inhibition of K^+ conductance, but the identities of the targeted channels have remained elusive.

The Ba^{2+} sensitivity, along with the electrophysiological characteristics (kinetics and voltage-dependence of activation, absence of time-dependent inactivation) of the A7r5 K_v current are similar to what has been described for the Kv7 family (KCNQ family) of voltage-gated K^+ channels (43). These channels are among the most recently identified mammalian K^+ channels and are thought to function in excitable cells to maintain a negative resting membrane potential. These channels have not historically been considered among the cohort of vascular ion channels, but recently, KCNQ channels were found to be expressed in murine portal vein (KCNQ1; Ref. 39), and functional vasoconstrictor effects of KCNQ channel blockers were demonstrated in rat and murine pulmonary arteries (28) and murine portal vein (60). No previous studies have demonstrated regulation of these channels by vasoconstrictor hormones.

Inhibition of K_v currents and vasoconstrictor actions of the selective KCNQ channel blockers linopirdine and XE991 have been the basis for postulating a functional role for KCNQ channels in rat and murine pulmonary arteries and portal vein (28,39,60). We have found that these same agents inhibit the AVP-sensitive K_v current in A7r5 cells at concentrations that selectively block KCNQ currents in other cells and that linopirdine mimics AVP in the stimulation of action potential generation and Ca^{2+} spiking. We also found that the KCNQ channel activator flupirtine has the opposite effect (increasing K_v current and suppressing AVP-stimulated Ca^{2+} spiking). KCNQ5 expression in A7r5 cells (and freshly isolated rat aortic smooth muscle cells) was confirmed by RT-PCR (whereas KCNQ1–4 were undetectable), and RNA interference targeted to KCNQ5 significantly decreased I_{Kv}. On the basis of these observations, we conclude that KCNQ5 channel inhibition mediates the stimulation of Ca^{2+} spiking via physiological concentrations of AVP in A7r5 cells.

KCNQ5 expression has been demonstrated in a number of brain regions as well as in sympathetic ganglia and skeletal muscle (35,48), but this is the first demonstration of its expression or function in vascular smooth muscle cells. KCNQ5 channel function has been measured using expression systems in which KCNQ5 overexpression yields currents with characteristics reminiscent of neuronal M currents and regulation by M1 muscarinic receptor activation (48). These properties are similar to the electrophysiological characteristics of K_v currents in A7r5 cells and their regulation by activation of V_{1a} vasopressin receptors. The signal transduction pathways involved in regulation of neuronal KCNQ5 currents by G protein-coupled receptor activation are not fully understood, but both hydrolysis of phosphatidylinositol 4,5-bisphosphate and activation of PKC have been implicated (11).

Is there any relationship between regulation of KCNQ5 and Kv1.2 channels by AVP? A role for Kv1.2 channels in A7r5 cells was suggested by our previous finding that AVP-induced Ca^{2+} spiking was dependent on PYK2 activation and the associated tyrosine phosphorylation of the Kv1.2 channel protein (3). M1 muscarinic acetylcholine receptor activation can also induce PYK2-dependent tyrosine phosphorylation of Kv1.2 channels and suppression of their activity (16,25). These findings suggest that M1 receptor activation can initiate the same signaling sequence that we previously implicated for AVP-stimulated Ca^{2+} spiking in A7r5 cells. As noted above, KCNQ5-mediated M currents also were suppressed in response to M1 receptor activation (48). Both KCNQ channels and Kv1.2 channels are widely distributed in neural tissues (11,50). If these channels coexist in neurons, their regulation by M1 receptor activation may represent a coordinated response in the stimulation of neuronal excitability. Although the relationship between KCNQ5 and Kv1.2 regulation in A7r5 cells is not completely clear, we may speculate that they are both involved in the regulation of excitability in vascular smooth muscle cells.

In summary, at physiological vasoconstrictor concentrations, AVP stimulates action potential generation and Ca^{2+} spiking in A7r5 cells via PKC-dependent inhibition of K_v currents. The latter have pharmacological and electrophysiological attributes of KCNQ5 channel currents, and the current amplitudes are decreased by knocking down KCNQ5 expression. Future studies are needed to examine the hypothesis that KCNQ5 channels are mediators in the physiological vasoconstrictor effects of vasopressin and potential targets for therapeutic intervention in cardiovascular diseases.

Acknowledgements

We gratefully acknowledge the technical assistance of Chris Hill. We also thank Merck Research Laboratories for providing correolide for use in these studies.

GRANTS

This work was supported by the Eugene J. and Elsie E. Weyler Endowment for Clinical Cardiology Research, the John and Marian Falk Trust for Medical Research, and National Heart, Lung, and Blood Institute Grants R01 HL-60164 and R01 HL-070670 (to K. L. Byron).

References

1. Beisel KW, Rocha-Sanchez SM, Morris KA, Nie L, Feng F, Kachar B, Yamoah EN, Fritzsch B. Differential expression of KCNQ4 in inner hair cells and sensory neurons is the basis of progressive high-frequency hearing loss. J Neurosci 2005;25:9285–93. [PubMed: 16207888]
2. Betts LC, Kozlowski RZ. Electrophysiological effects of endothelin-1 and their relationship to contraction in rat renal arterial smooth muscle. Br J Pharmacol 2000;130:787–796. [PubMed: 10864884]
3. Byron KL, Lucchesi PA. Signal transduction of physiological concentrations of vasopressin in A7r5 vascular smooth muscle cells. J Biol Chem 2002;277:7298–7307. [PubMed: 11739373]
4. Byron KL, Villereal ML. Mitogen-induced $[Ca^{2+}]_i$ changes in individual human fibroblasts. Image analysis reveals asynchronous responses which are characteristic for different mitogens. J Biol Chem 1989;264:18234–18239. [PubMed: 2808375]
5. Byron KL. Vasopressin stimulates Ca^{2+} spiking activity in A7r5 vascular smooth muscle cells via activation of phospholipase A_2. Circ Res 1996;78:813–820. [PubMed: 8620601]
6. Brueggemann LI, Markun DR, Henderson KK, Cribbs LL, Byron KL. Pharmacological and electrophysiological characterization of store-operated currents and capacitative Ca^{2+} entry in vascular smooth muscle cells. J Pharmacol Exp Ther 2006;317:488–499. [PubMed: 16415091]
7. Cheong A, Dedman AM, Beech DJ. Expression and function of native potassium channel ($K_V\alpha1$) subunits in terminal arterioles of rabbit. J Physiol 2001;534:691–700. [PubMed: 11483700]
8. Clément-Chomienne O, Walsh MP, Cole WC. Angiotensin II activation of protein kinase C decreases delayed rectifier K^+ current in rabbit vascular myocytes. J Physiol 1996;495:689–700. [PubMed: 8887776]
9. Cox RH. Molecular determinants of voltage-gated potassium currents in vascular smooth muscle. Cell Biochem Biophys 2005;42:167–195. [PubMed: 15858231]
10. Dai Y, Zhang JH. Role of Cl^- current in endothelin-1-induced contraction in rabbit basilar artery. Am J Physiol Heart Circ Physiol 2001;281:H2159–H2167. [PubMed: 11668078]
11. Delmas P, Brown DA. Pathways modulating neural KCNQ/M (Kv7) potassium channels. Nat Rev Neurosci 2005;6:850–862. [PubMed: 16261179]
12. Dumont E, Lamontagne D. No role of ATP-sensitive potassium channels in the vasoconstriction produced by vasopressin. J Vasc Res 1995;32:138–142. [PubMed: 7734660]
13. Ellershaw DC, Greenwood IA, Large WA. Modulation of volume-sensitive chloride current by noradrenaline in rabbit portal vein myocytes. J Physiol 2002;542:537–547. [PubMed: 12122151]
14. Fan J, Byron KL. Ca^{2+} signalling in rat vascular smooth muscle cells: a role for protein kinase C at physiological vasoconstrictor concentrations of vasopressin. J Physiol 2000;524:821–831. [PubMed: 10790161]

15. Felix JP, Bugianesi RM, Schmalhofer WA, Borris R, Goetz MA, Hensens OD, Bao JM, Kayser F, Parsons WH, Rupprecht K, Garcia ML, Kaczorowski GJ, Slaughter RS. Identification and biochemical characterization of a novel nortriterpene inhibitor of the human lymphocyte voltage-gated potassium channel, Kv1.3. Biochemistry 1999;38:4922–4930. [PubMed: 10213593]
16. Felsch JS, Cachero TG, Peralta EG. Activation of protein tyrosine kinase PYK2 by the m1 muscarinic acetylcholine receptor. Proc Natl Acad Sci USA 1998;95:5051–5056. [PubMed: 9560226]
17. Gokina NI, Bevan RD, Walters CL, Bevan JA. Electrical activity underlying rhythmic contraction in human pial arteries. Circ Res 1996;78:148–151. [PubMed: 8603497]
18. Grynkiewicz G, Poenie M, Tsien RY. A new generation of Ca^{2+} indicators with greatly improved fluorescence properties. J Biol Chem 1985;260:3440–3450. [PubMed: 3838314]
19. Guibert C, Beech DJ. Positive and negative coupling of the endothelin ET_A receptor to Ca^{2+}-permeable channels in rabbit cerebral cortex arterioles. J Physiol 1999;514:843–856. [PubMed: 9882755]
20. Guibert C, Marthan R, Savineau JP. Oscillatory Cl^- current induced by angiotensin II in rat pulmonary arterial myocytes: Ca^{2+} dependence and physiological implication. Cell Calcium 1997;21:421–429. [PubMed: 9223678]
21. Hanner M, Schmalhofer WA, Green B, Bordallo C, Liu J, Slaughter RS, Kaczorowski GJ, Garcia ML. Binding of correolide to K_v1 family potassium channels. Mapping the domains of high affinity interaction. J Biol Chem 1999;274:25237–25244. [PubMed: 10464244]
22. Harder DR, Sperelakis N. Membrane electrical properties of vascular smooth muscle from the guinea pig superior mesenteric artery. Pflügers Arch 1978;378:111–119.
23. Harder DR, Sperelakis N. Action potential generation in reaggregates of rat aortic smooth muscle cells in primary culture. Blood Vessels 1979;16:186–201. [PubMed: 454857]
24. Hayabuchi Y, Standen NB, Davies NW. Angiotensin II inhibits and alters kinetics of voltage-gated K^+ channels of rat arterial smooth muscle. Am J Physiol Heart Circ Physiol 2001;281:H2480–H2489. [PubMed: 11709415]
25. Huang XY, Morielli AD, Peralta EG. Tyrosine kinase-dependent suppression of a potassium channel by the G protein-coupled m1 muscarinic acetylcholine receptor. Cell 1993;75:1145–1156. [PubMed: 8261514]
26. Iwasawa K, Nakajima T, Hazama H, Goto A, Shin WS, Toyooka T, Omata M. Effects of extracellular pH on receptor-mediated Ca^{2+} influx in A7r5 rat smooth muscle cells: involvement of two different types of channel. J Physiol 1997;503:237–251. [PubMed: 9306269]
27. Jackson WF. Ion channels and vascular tone. Hypertension 2000;35:173–178. [PubMed: 10642294]
28. Joshi S, Balan P, Gurney AM. Pulmonary vasoconstrictor action of KCNQ potassium channel blockers. Respir Res 2006;20:7–31.
29. Jung S, Strotmann R, Schultz G, Plant T. TRPC6 is a candidate channel involved in receptor-stimulated cation currents in A7r5 smooth muscle cells. Am J Physiol Cell Physiol 2002;282:C347–C359. [PubMed: 11788346]
30. Kitamura K, Yamazaki J. Chloride channels and their functional roles in smooth muscle tone in the vasculature. Jpn J Pharmacol 2001;85:351–357. [PubMed: 11388637]
31. Krautwurst D, Degtiar VE, Schultz G, Hescheler J. The isoquinoline derivative LOE 908 selectively blocks vasopressin-activated nonselective cation currents in A7r5 aortic smooth muscle cells. Naunyn Schmiedebergs Arch Pharmacol 1994;349:301–307. [PubMed: 7516040]
32. Lamb FS, Barna TJ. Chloride ion currents contribute functionally to norepinephrine-induced vascular contraction. Am J Physiol Heart Circ Physiol 1998;275:H151–H160.
33. Lamb FS, Kooy NW, Lewis SJ. Role of Cl^- channels in α-adrenoceptor-mediated vasoconstriction in the anesthetized rat. Eur J Pharmacol 2000;401:403–412. [PubMed: 10936500]
34. Large WA. Receptor-operated Ca^{2+}-permeable nonselective cation channels in vascular smooth muscle: a physiologic perspective. J Cardiovasc Electrophysiol 2002;13:493–501. [PubMed: 12030534]
35. Lerche C, Scherer CR, Seebohm G, Derst C, Wei AD, Busch AE, Steinmeyer K. Molecular cloning and functional expression of KCNQ5, a potassium channel subunit that may contribute to neuronal M-current diversity. J Biol Chem 2000;275:22395–22400. [PubMed: 10787416]

36. Li KX, Fouty B, McMurtry IF, Rodman DM. Enhanced ET_A-receptor-mediated inhibition of K_v channels in hypoxic hypertensive rat pulmonary artery myocytes. Am J Physiol Heart Circ Physiol 1999;277:H363–H370.
37. Nakajima T, Hazama H, Hamada E, Wu SN, Igarashi K, Yamashita T, Seyama Y, Omata M, Kurachi Y. Endothelin-1 and vasopressin activate Ca^{2+}-permeable non-selective cation channels in aortic smooth muscle cells: mechanism of receptor-mediated Ca^{2+} influx. J Mol Cell Cardiol 1996;28:707–722. [PubMed: 8732499]
38. Nelson MT, Quayle JM. Physiological roles and properties of potassium channels in arterial smooth muscle. Am J Physiol Cell Physiol 1995;268:C799–C822.
39. Ohya S, Sergeant GP, Greenwood IA, Horowitz B. Molecular variants of KCNQ channels expressed in murine portal vein myocytes: a role in delayed rectifier current. Circ Res 2003;92:1016–1023. [PubMed: 12690036]
40. Passmore GM, Selyanko AA, Mistry M, Al-Qatari M, Marsh SJ, Matthews EA, Dickenson AH, Brown TA, Burbidge SA, Main M, Brown DA. KCNQ/M currents in sensory neurons: significance for pain therapy. J Neurosci 2003;23:7227–7236. [PubMed: 12904483]
41. Petkova-Kirova P, Gagov H, Krien U, Duridanova D, Noack T, Schubert R. 4-Aminopyridine affects rat arterial smooth muscle BK_{Ca} currents by changing intracellular pH. Br J Pharmacol 2000;131:1643–50. [PubMed: 11139442]
42. Prior HM, Yates MS, Beech DJ. Functions of large conductance Ca^{2+}-activated (BK_{Ca}), delayed rectifier (K_V) and background K^+ channels in the control of membrane potential in rabbit renal arcuate artery. J Physiol 1998;511:159–169. [PubMed: 9679171]
43. Robbins J. KCNQ potassium channels: physiology, pathophysiology, and pharmacology. Pharmacol Ther 2001;90:1–19. [PubMed: 11448722]
44. Salter KJ, Kozlowski RZ. Endothelin receptor coupling to potassium and chloride channels in isolated rat pulmonary arterial myocytes. J Pharmacol Exp Ther 1996;279:1053–1062. [PubMed: 8930216]
45. Salter KJ, Turner JL, Albarwani S, Clapp LH, Kozlowski RZ. Ca^{2+}-activated Cl^- and K^+ channels and their modulation by endothelin-1 in rat pulmonary arterial smooth muscle cells. Exp Physiol 1995;80:815–824. [PubMed: 8546870]
46. Salter KJ, Wilson CM, Kato K, Kozlowski RZ. Endothelin-1, delayed rectifier K channels, and pulmonary arterial smooth muscle. J Cardiovasc Pharmacol 1998;31:S81–S83. [PubMed: 9595407]
47. Schilling WP. TRP proteins: novel therapeutic targets for regional blood pressure control? Circ Res 2001;88:256–259. [PubMed: 11179189]
48. Schroeder BC, Hechenberger M, Weinreich F, Kubisch C, Jentsch TJ. KCNQ5, a novel potassium channel broadly expressed in brain, mediates M-type currents. J Biol Chem 2000;275:24089–24095. [PubMed: 10816588]
49. Serir K, Hayoz S, Fanchaouy M, Jean-Louis Beny JL, Bychkov R. A delayed ATP-elicited K^+ current in freshly isolated smooth muscle cells from mouse aorta. Br J Pharmacol 2006;147:45–54. [PubMed: 16258525]
50. Sheng M, Tsaur ML, Jan YN, Jan LY. Contrasting subcellular localization of the Kv1.2 K^+ channel subunit in different neurons of rat brain. J Neurosci 1994;14:2408–2417. [PubMed: 8158277]
51. Shimoda LA, Sylvester JT, Sham JS. Inhibition of voltage-gated K^+ current in rat intrapulmonary arterial myocytes by endothelin-1. Am J Physiol Lung Cell Mol Physiol 1998;274:L842–L853.
52. Shimoda LA, Sylvester JT, Booth GM, Shimoda TH, Meeker S, Undem BJ, Sham JS. Inhibition of voltage-gated K^+ currents by endothelin-1 in human pulmonary arterial myocytes. Am J Physiol Lung Cell Mol Physiol 2001;281:L1115–L1122. [PubMed: 11597902]
53. Si H, Grgic I, Heyken WT, Maier T, Hoyer J, Reusch HP, Kohler R. Mitogenic modulation of Ca^{2+}-activated K^+ channels in proliferating A7r5 vascular smooth muscle cells. Br J Pharmacol. June 12;2006 10.1038/sj.bjp.0706793
54. Stevens T. Is there a role for store-operated calcium entry in vasoconstriction? Am J Physiol Lung Cell Mol Physiol 2001;280:L866–L869. [PubMed: 11290509]
55. Tammaro P, Smith AL, Hutchings SR, Smirnov SV. Pharmacological evidence for a key role of voltage-gated K^+ channels in the function of rat aortic smooth muscle cells. Br J Pharmacol 2004;143:303–317. [PubMed: 15326038]

56. Van Renterghem C, Lazdunski M. Endothelin and vasopressin activate low conductance chloride channels in aortic smooth muscle cells. Pflügers Arch 1993;425:156–163.
57. Van Renterghem C, Lazdunski M. A small-conductance charybdotoxin-sensitive, apamin-resistant Ca^{2+}-activated K^{+} channel in aortic smooth muscle cells (A7r5 line and primary culture). Pflügers Arch 1992;420:417–423.
58. Van Renterghem C, Romey G, Lazdunski M. Vasopressin modulates the spontaneous electrical activity in aortic cells (line A7r5) by acting on three different types of ionic channels. Proc Natl Acad Sci USA 1988;85:9365–9369. [PubMed: 2461570]
59. Wong KL, Chan P, Huang WC, Yang TL, Liu IM, Lai TY, Tsai CC, Cheng JT. Effect of tetramethylpyrazine on potassium channels to lower calcium concentration in cultured aortic smooth muscle cells. Clin Exp Pharmacol Physiol 2003;30:793–798. [PubMed: 14516420]
60. Yeung SY, Greenwood IA. Electrophysiological and functional effects of the KCNQ channel blocker XE991 on murine portal vein smooth muscle cells. Br J Pharmacol 2005;146:585–595. [PubMed: 16056238]

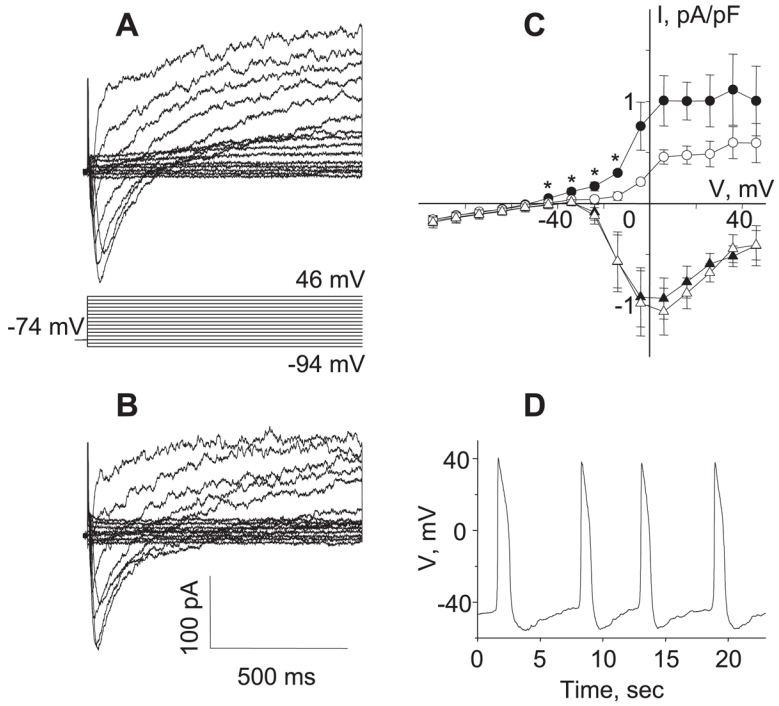

Fig. 1.

Inhibition of K^+ currents in a single A7r5 cell by AVP triggers action potential (AP) generation. *A* and *B*: original current traces recorded in a single A7r5 cell before (*A*) and after (*B*) application of 100 pM AVP for 10 min. Step voltage protocol is shown in *A*. *C*: sustained outward currents were evaluated by averaging 1,000 points collected over the last 100 ms of the voltage pulse, and L-type Ca^{2+} currents were evaluated by measuring the peak inward current. Mean current recorded at the end of the pulse (circles) and peak current recorded at the beginning of the pulse (triangles) in control (filled symbols) and after application of 100 pM AVP (open symbols) are shown ($n = 5$). *I*, current; *V*, voltage. *$P < 0.05$, statistically significant differences from control (Student's *t*-test). *D*: APs stimulated by 100 pM AVP, recorded in the same cell in current-clamp mode. Similar results were obtained in 6 experiments.

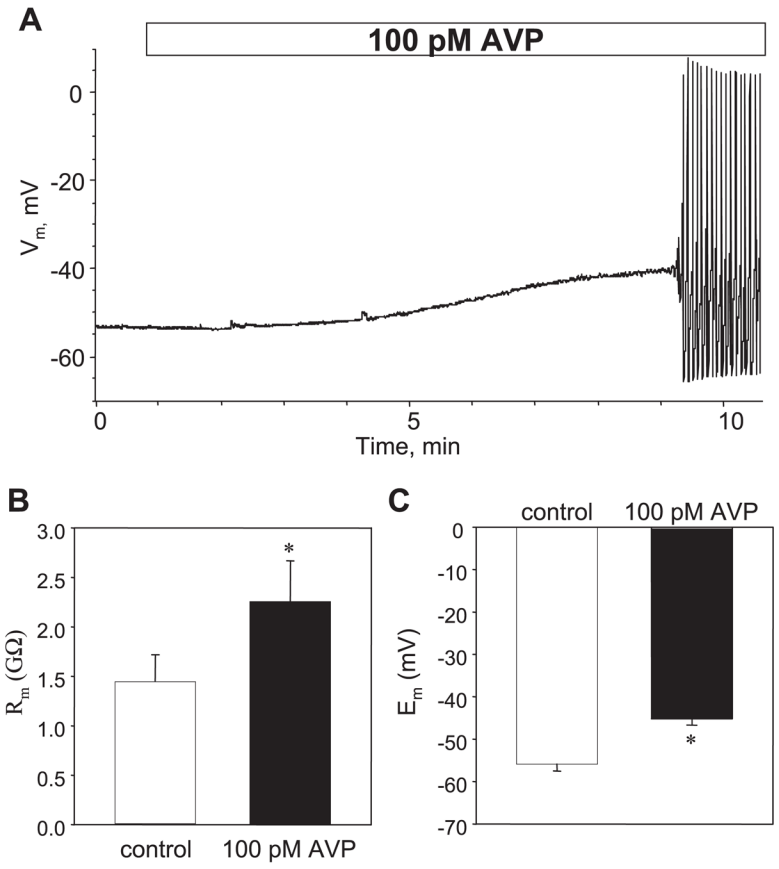

Fig. 2.

Membrane depolarization by AVP is associated with an increase in membrane resistance (R_m). *A*: representative trace shows time course of AP activation in a single A7r5 cell treated with 100 pM AVP. Note membrane depolarization prior to AP generation. Similar results were obtained in 6 experiments; mean time to initiation of AP firing was 5.7 ± 0.8 min (n = 6). V_m, membrane potential. *B*: application of 100 pM AVP significantly increased R_m from 1.44 ± 0.27 to 2.26 ± 0.41 GΩ (n = 7, P = 0.005, paired t-test) as calculated from the currents measured in response to 20-mV voltage steps from −64 to −44 mV (±10 mV from the resting membrane potential, E_m). *C*: in the same time frame, application of 100 pM AVP significantly depolarized the membrane from −55.9 ± 1.6 to −45.2 ± 1.4 mV (n = 8, P < 0.001).

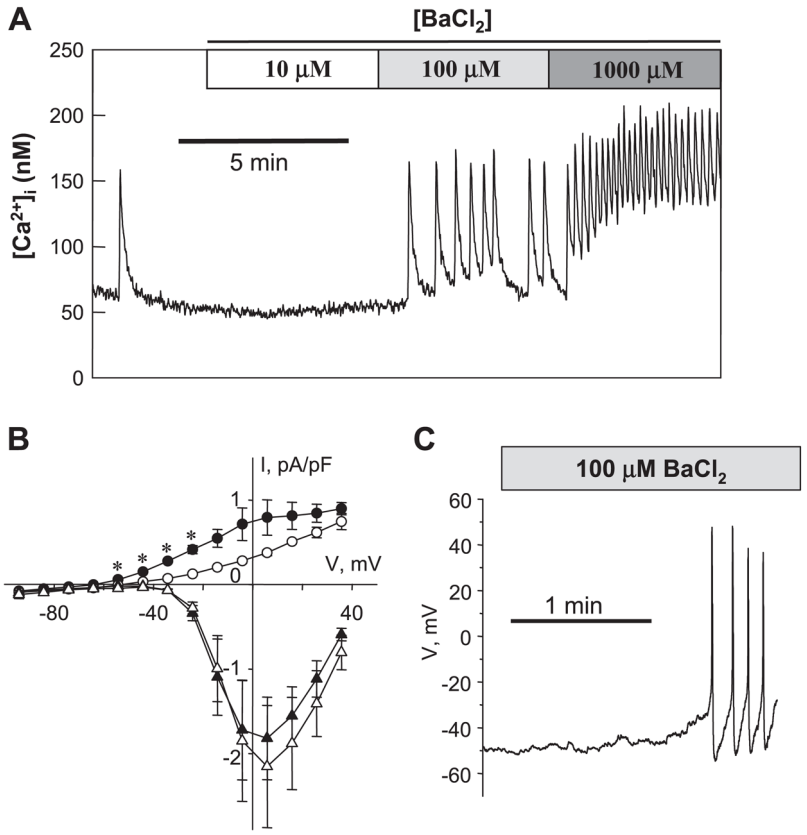

Fig. 3.

K^+ channel blocker $BaCl_2$ mimics AVP in inhibition of K_v currents, stimulation of AP firing, and Ca^{2+} spiking. *A*: Ca^{2+} spiking activity (intracellular Ca^{2+} concentration, $[Ca^{2+}]_i$) in a population of A7r5 cells in response to $BaCl_2$, a nonselective K^+ channel blocker (representative of 5 similar experiments). Similar to AVP, 100 μM $BaCl_2$ inhibits outward K^+ current and activates AP firing. *B*: mean current recorded at the end of the pulse (circles) and peak current recorded at the beginning of the pulse (triangles) in control (filled symbols) and in the presence of 100 μM $BaCl_2$ (open symbols). Data are presented as means ± SE, n = 5. *$P < 0.05$, statistically significant differences from the control (paired Student's t-test). *C*: representative trace of V_m recorded in current-clamp mode showing stimulation of AP generation by 100 μM $BaCl_2$ in a single A7r5 cell.

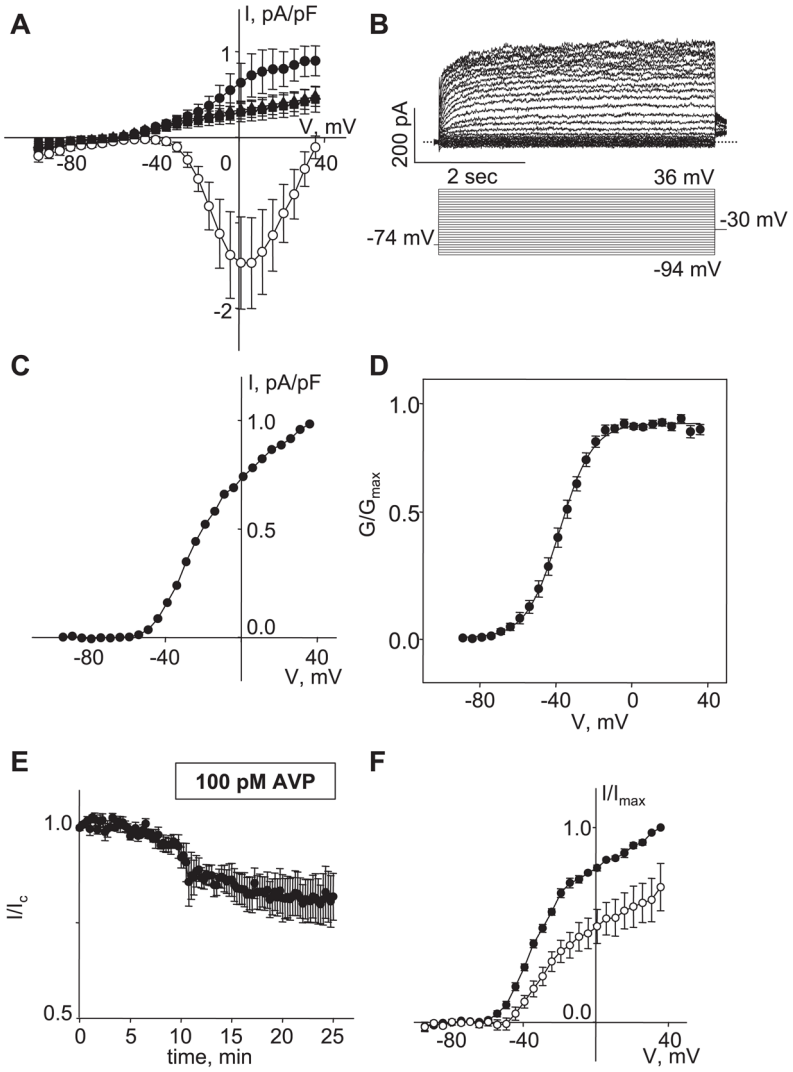

Fig. 4.

Isolation of AVP-sensitive K_v currents in single A7r5 cells. *A*: mean current recorded at the end of the pulse (●) and peak inward current recorded at the beginning of the pulse in control (○) followed by application of 10 μM verapamil plus 100 nM iberiotoxin for 10 min (▲). Verapamil and iberiotoxin were then replaced with 100 μM $GdCl_3$ (▪) for an additional 10 min (n = 4). Peak inward currents recorded in the presence of verapamil plus iberiotoxin and $GdCl_3$ were omitted for clarity. *B*: representative traces of current recorded in the presence of 100 μM $GdCl_3$ in external solution to isolate K_v component (*top*). With a holding potential of −74 mV, a voltage step protocol was applied to test potentials from −94 to +36 mV, followed by steps to −30 mV for tail-current recording. Dotted line indicates 0 current level. *C*: mean current recorded at the end of the pulse (1,000 points recorded over the last 500 ms were averaged) from the traces presented in *B* after leak subtraction and normalization to the cell capacitance (C = 284 pF). *D*: voltage dependence of steady-state activation fitted by the single Boltzmann function (solid line, see Materials and Methods). Conductance was calculated from the tail currents measured at −30 mV based on a K^+ reversal potential of −84 mV. Voltage of half-maximal activation ($V_{0.5}$) = −38.0 ± 1.6 mV; slope factor (s) −8.3 ± 0.4 mV (n = 21); G/G_{max}, fractional maximal conductance. *E*: time course of K_v current inhibition by 100 pM AVP recorded by applying a 5-s step to a membrane potential of 0 mV from a holding potential of

−74 mV at 15-s intervals. Currents were normalized to mean control current (I/I_c) recorded for 10 min before adding AVP ($n = 7$). *F: I-V* curves of mean outward current measured in the presence of 100 μM Gd^{3+} in control and after exposure to 100 pM AVP for 15 min. After leak subtraction, currents were normalized to the maximal control current (I/I_{max}; ●) measured at −36 mV. AVP significantly reduced K_v current at all membrane potentials from −54 to +36 mV ($n = 7$, $P < 0.05$, paired Student's *t*-test).

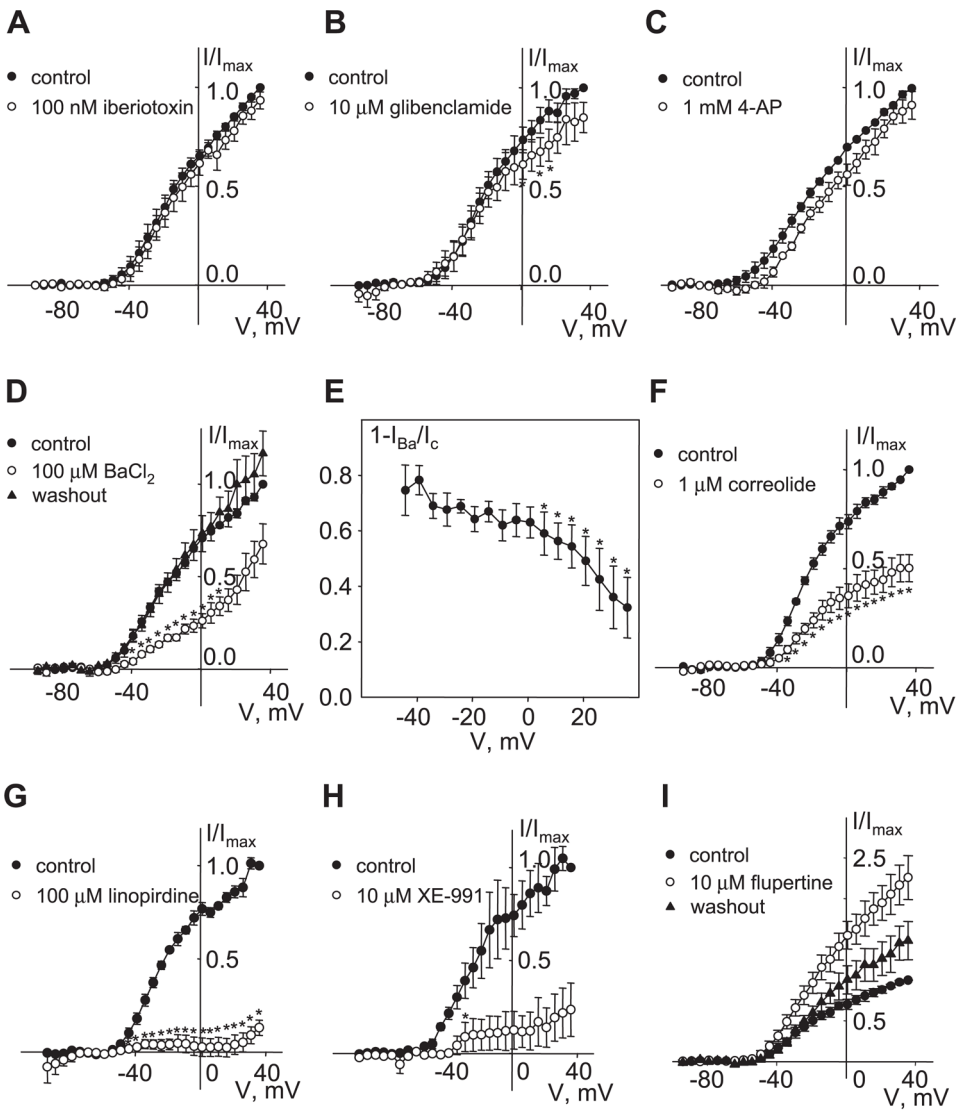

Fig. 5.

Pharmacology of K_v current. *I-V* curves of mean outward current were measured as described in Fig. 4 legend in the presence of 100 μM Gd^{3+}. After leak subtraction, currents were normalized to the maximal control current measured at 36 mV. Currents were measured in the presence of 100 nM iberiotoxin (*A; n* = 4), 10 μM glibenclamide (*B; n* = 3), 1 mM 4-aminopyridine (4-AP; *C; n* = 3), 100 μM $BaCl_2$ followed by washout (*D; n* = 5), 1 μM correolide (*F; n* = 4), 100 μM linopirdine (*G; n* = 3), 10 μM XE-991 (*H; n* = 3), and 10 μM flupirtine followed by washout (*I; n* = 4). **P* < 0.05, statistically significant difference from control (paired Student's *t*-test). *E*: inhibition of K_v current by Ba^{2+} was voltage dependent. Currents recorded in the presence of 100 μM Ba^{2+}(I_{Ba}) were reduced compared with control current (I_c) by 75 ± 9% at −44 mV and by 32 ± 11% at +36 mV. **P* < 0.05, statistically significant difference from inhibition at −44 mV [1-way repeated-measures ANOVA (Holm-Sidak method)]. Data are presented as means ± SE.

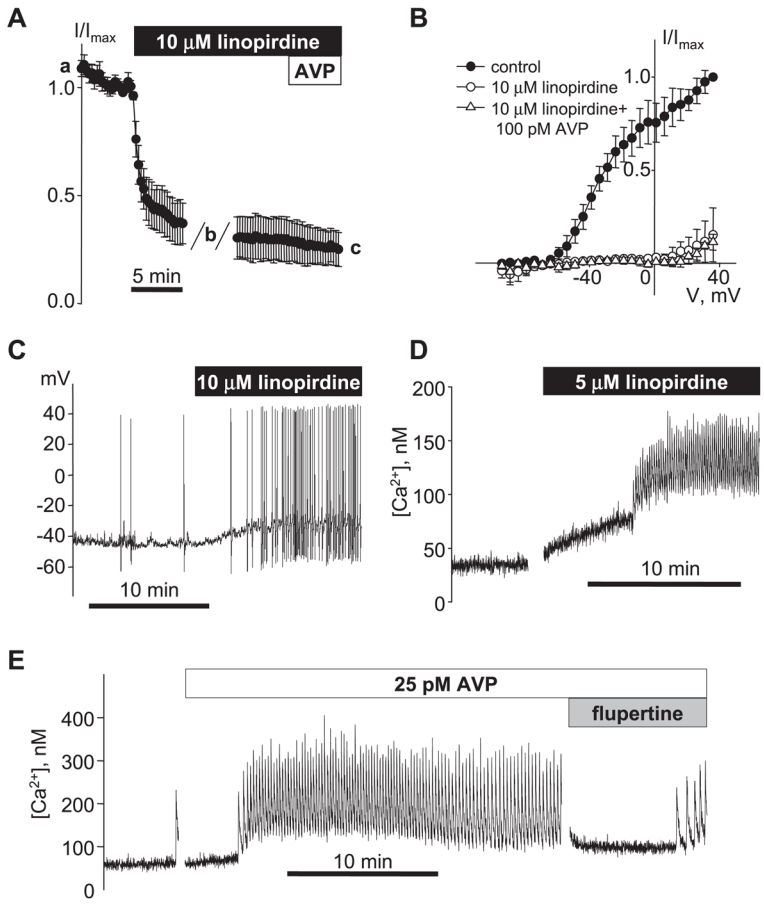

Fig. 6.

Effects of KCNQ channel blockers/activators on A7r5 cell excitability. *A*: mean time course for inhibition of I_{Kv} by 10 μM linopirdine was measured as described for 100 pM AVP in Fig. 4*E* (n = 3). AVP (100 pM) was added to the bath after 15-min treatment with linopirdine. *B: I-V* curves (after leak subtraction; mean of 3) recorded before, during 10 μM linopirdine treatment, and after 5-min exposure to 100 pM AVP in the continued presence of linopirdine (time points indicated by *a*, *b*, and *c*, respectively, in *A*). *C*: representative trace of membrane potential recorded in current-clamp mode showing stimulation of AP generation by 10 μM linopirdine in a single A7r5 cell. *D*: stimulation of Ca^{2+} spiking activity by 5 μM linopirdine in a population of A7r5 cells (representative of 4 similar experiments with concentrations of linopirdine between 1 and 10 μM). *E*: AVP-induced Ca^{2+} spiking activity was transiently reversed by application of 10 μM flupirtine (representative of 3 similar experiments).

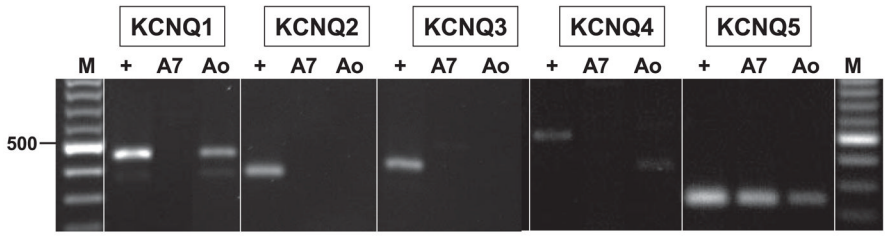

Fig. 7.

Expression of KCNQ isoforms in A7r5 cells and adult rat aorta. Total RNA prepared from A7r5 cells (A7), adult rat thoracic aorta (Ao), or adult rat brain as a positive control (+) was reverse transcribed and subjected to PCR using primers specific for KCNQ1 through KCNQ5. Molecular weight marker (M) is a 100-bp ladder; 500 bp is indicated at *left*. Expected sizes of reaction products are KCNQ1, 453 bp; KCNQ2, 372 bp; KCNQ3, 424 bp; KCNQ4, 495 bp; and KCNQ5, 240 bp. Products were confirmed by DNA sequencing.

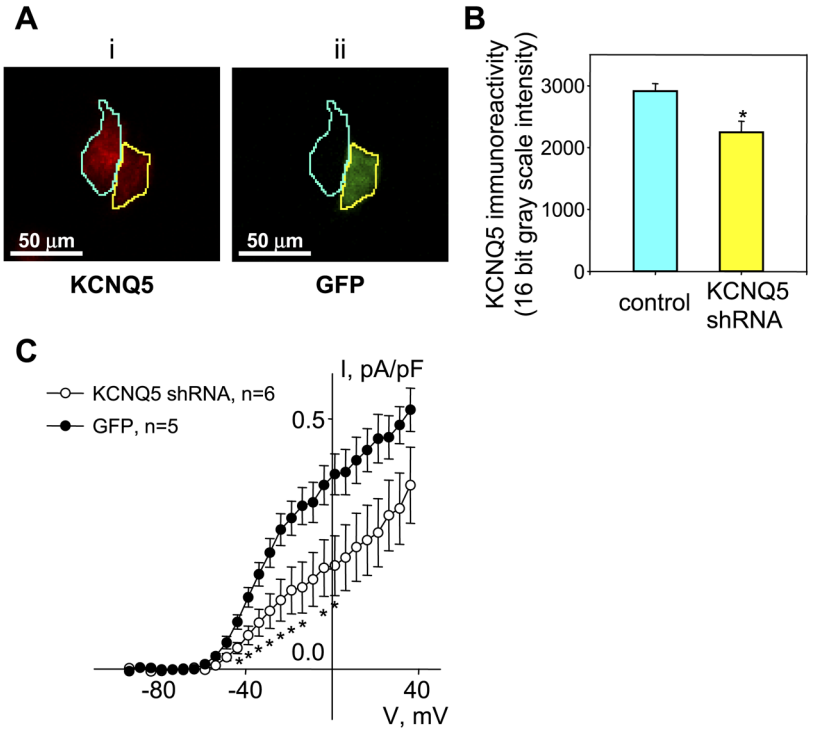

Fig. 8.

KCNQ5 short hairpin (sh)RNA reduces KCNQ5 expression and K_v currents in A7r5 cells. *A*: KCNQ5 protein expression in A7r5 cells infected with lentiviral vectors for expression of KCNQ5 shRNA (lv-GFP_KCNQ5-shRNA) was detected by immunohistochemical analysis using rabbit polyclonal anti-KCNQ5 antibodies and an Alexa Fluor 594-conjugated goat anti-rabbit IgG secondary antibody (*i*). Green fluorescent protein (GFP) was used as an indication of expression of the KCNQ5 shRNA construct (*ii*; GFP-expressing cell outlined in yellow in both images; control cell without GFP fluorescence outlined in cyan in both images). Cells expressing GFP displayed reduced KCNQ5 immunoreactivity. *B*: quantitative image analysis of 128 cells, comparing KCNQ5 immunoreactivity in cells expressing KCNQ5 shRNA or non-GFP-expressing control cells in the same cultures. **P* < 0.05, significant difference from control (Student's *t*-test). *C: I-V* curves of mean outward current (measured as described in Fig. 4 legend in the presence of 100 μM Gd^{3+}) after leak subtraction and normalization to the cell capacitance. K_V currents were measured in GFP-fluorescent A7r5 cells from parallel cultures infected with lv-GFP_KCNQ5-shRNA (*n* = 6) or GFP alone (*n* = 5). In the voltage range from −44 to −1 mV, K_v currents were significantly reduced (by ~50%) in lv-KCNQ5_shRNA-infected cells (*P* < 0.05, unpaired Student's *t*-test).

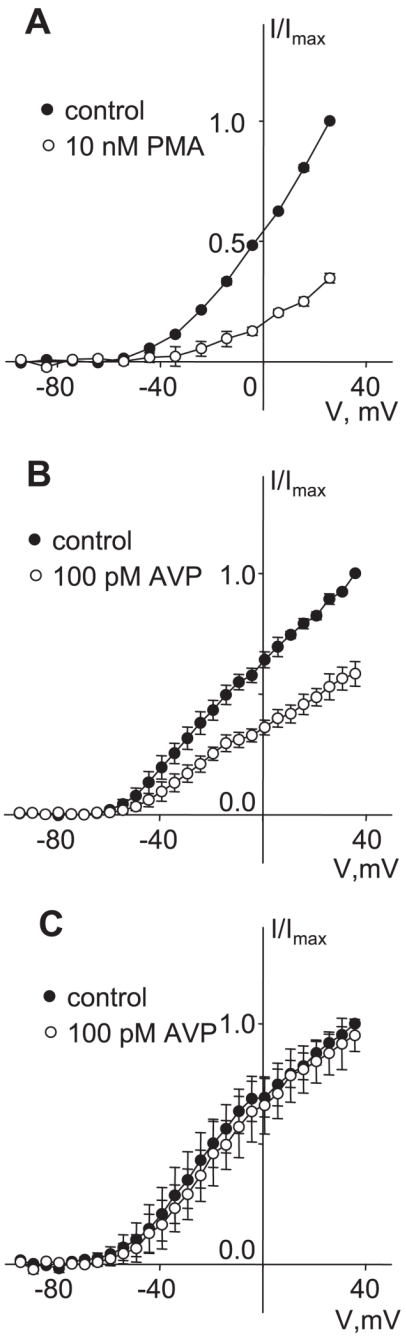

Fig. 9.

PKC dependence of K_v currents. *A: I-V* curves of mean currents recorded at the end of voltage pulses in control and after application of 10 nM PMA for 10 min. After leak subtraction, currents were normalized to the maximal control current measured at −36 mV, and data are presented as means ± SE (n = 3). *B: I-V* curves of mean currents recorded at the end of voltage pulses before (control) and after AVP application for 10 min. Currents were normalized to the maximal control current measured at 36 mV, and data are presented as means ± SE (n = 3). *C*: a similar series of experiments was conducted in cells pretreated for 1 h with 250 nM calphostin C. Results are displayed as described in *B* (n = 3). All measurements for *A–C* were made in the presence of 100 μM $GdCl_3$ in the external solution.